Nanostructured Magnets for Improved Energy Efficiency

M.A. Willard,[1] K.E. Knipling,[1] and M. Daniil[2]
[1]*Materials Science and Technology Division*
[2]*George Washington University*

Introduction: Reducing our reliance on fossil fuels by the widespread hybrid and electric transportation options has resulted in a recent surge in sustainable energy research and infrastructure, especially in electricity generation from replenishable energy sources (e.g., wind, solar, hydro, and geothermal). In parallel with this infrastructure investment, it is also essential to develop technologies that avoid squandering these newly tapped resources by improving the efficiency of energy production, distribution, and consumption. By reducing the losses inherent to power generation, conditioning, and conversion, energy efficiency will be improved, adding to our overall energy sustainability. The Navy's effort to produce "all- electric ship" technologies requires improvements in these areas to achieve the highest possible shipboard power density. Significant gains can be achieved by development of smaller, lighter, and more efficient power converters and magnetic filters. A main challenge to the energy efficiency of these components is the loss generated by the magnetic core materials from hysteretic, acoustic, or eddy current sources. This article discusses NRL's alloy research regarding the fabrication and characterization of novel nanostructured soft magnetic alloys exhibiting low core losses and designed for use in power applications.

Nanotechnology Solution: Nanocrystalline soft magnetic alloys are a class of premiere magnetic materials exhibiting a large saturation magnetization and small coercivity, resulting in a highly efficient core material for alternating current applications.[1] These materials consist of nanoscale magnetic crystallites embedded within an intergranular amorphous matrix (schematically shown in Fig. 1). The partially crystalline material with refined grain size results in a desirable combination of large saturation induction, high permeability, and low core losses, unobtainable in conventional soft magnetic alloys. The improved performance is only possible when grains are smaller than a fundamental magnetic length scale called the exchange correlation length (L_{ex}) and the operation temperature is sufficiently low such that the magnetic coupling between grains is maintained. A current technical challenge is meeting both of these objectives in a cost-effective way.

Materials Processing: Achieving the optimal magnetic performance for energy efficiency and size/weight reduction requires non-equilibrium processing to achieve the necessary nanoscale microstructure. Two steps are used to prepare these materials. First, a rapid solidification process is used to create an amorphous alloy (i.e., material with disordered atomic-scale structure) in the form of long, thin ribbons. These materials are subsequently annealed above 500 °C to produce the ultrafine grains necessary for low core losses. Alloys with composition $(Fe_{1-2x}Co_xNi_x)_{88}Zr_7B_4Cu_1$ have been recently designed and produced at NRL using a single-wheel, melt-spinning process (see Fig. 2) in which a molten alloy of the desired composition is expelled through a jet-cast orifice onto a rapidly rotating copper wheel (~50 m/s), solidifying the melt at a rate exceeding 10^5 °C/s.

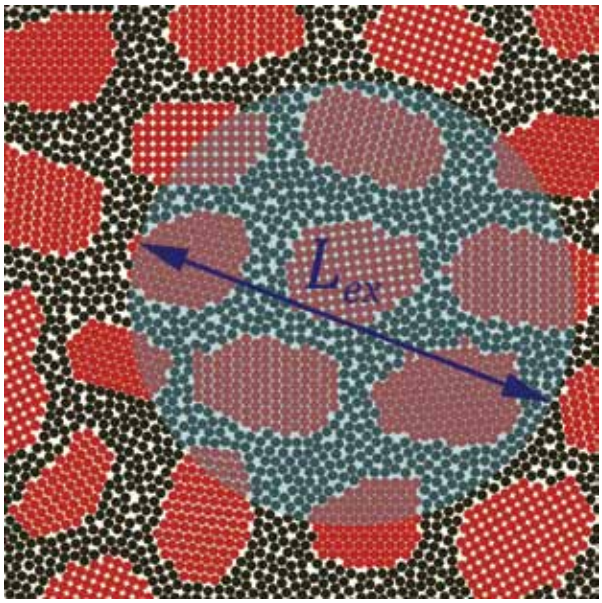

FIGURE 1
Schematic diagram showing relationship between nanocrystalline grains (red) and exchange correlation length (light blue).

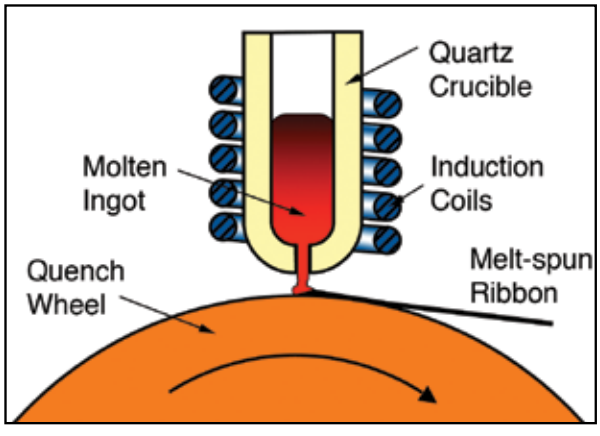

FIGURE 2
Schematic diagram of the melt-spinning technique for forming amorphous ribbons from a molten alloy.

Magnetic Performance: Due to their refined grain size and intergranular amorphous phase, these nanostructured alloys possess low hysteretic and core losses. Using state-of-the-art magnetometers at NRL, magnetic hysteresis loop measurements were collected at temperatures up to 600 °C (see Fig. 3). From these measurements, the important performance metrics — the saturation magnetization and the coercivity — were determined and compared with other soft magnets. Large values of saturation magnetization are desirable because less core material is required for a given flux density in application, while small values of coercivity result in lower losses and better energy efficiency. The magnetic properties of a state-of-the-art (Fe,Co)-based nanocrystalline material specifically designed for high-temperature applications is shown in Fig. 3. Our new alloys have comparable saturation magnetization values with much lower coercivity, resulting in improved energy efficiency. Moreover, the small Co content of the alloys improves the cost effectiveness considerably.

Summary: The newly developed nanocrystalline alloy, with composition $Fe_{77}Co_{5.5}Ni_{5.5}Zr_7B_4Cu_1$, shows improved losses through the broad temperature range from room temperature to 500 °C.[2] These materials are suitable for Naval power applications at frequencies up to 100 kHz and for use in high-temperature environments or at room temperatures without the necessity for oil cooling (i.e., green technology).

[Sponsored by ONR]

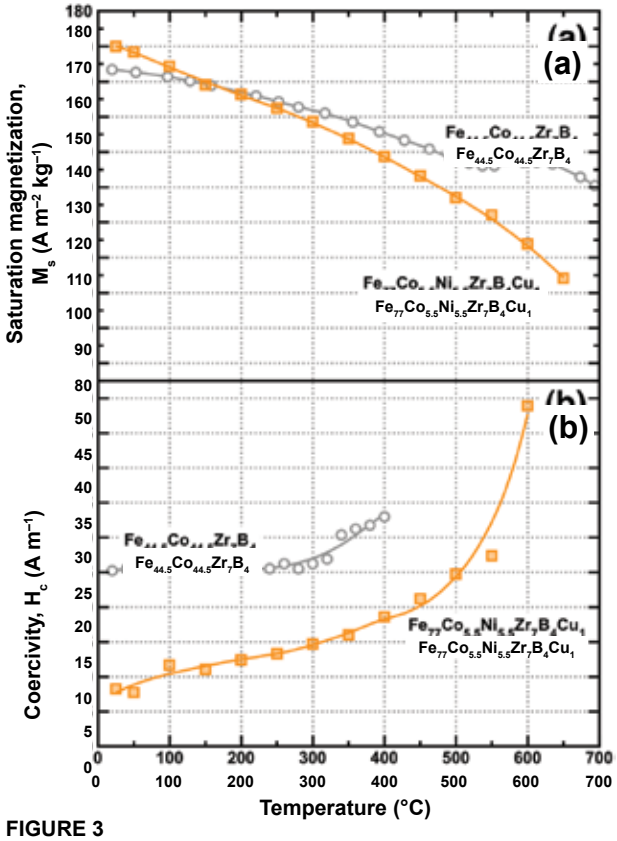

FIGURE 3
Temperature dependence of (a) saturation magnetization and (b) coercivity for a nanocrystalline alloy developed at NRL ($Fe_{77}Co_{5.5}Ni_{5.5}Zr_7B_4Cu_1$) and a state-of-the-art alloy designed for high-temperature use ($Fe_{44.5}Co_{44.5}Zr_7B_4$).[2]

References

[1] M.A. Willard and M. Daniil, "Nanostructured Soft Magnetic Materials," in *Nanoscale Magnetic Materials and Applications,* eds. J.P. Liu et al. (Springer, New York, 2009) pp. 373–398.

[2] K. Knipling, M. Daniil, and M.A. Willard, "Fe-based Nanocrystalline Soft Magnetic Alloys for High Temperature Applications," *Appl. Phys. Lett.* **95**, 222516 (2009); I. Skorvanek et al., *Phys. Status Solidi A* **196**, 217–220 (2003).

High Performance Antireflection Structured IR Fibers

J.S. Sanghera,[1] C. Florea,[2] L.E. Busse,[1] L.B. Shaw,[1] F.H. Kung,[3] and I.D. Aggarwal[1]

[1]*Materials Science and Technology Division*
[2]*Global Defense Technology & Systems, Inc.*
[3]*University Research Foundation*

The Problem: Infrared optical fibers are being developed for numerous applications in the 2 to 12 μm wavelength region. These include laser power delivery for infrared missile protection systems as well as infrared active devices such as lasers, filters, and wavelength converters. However, the choice of materials that can be used to draw optical fibers for this region is limited to high-index materials, such as chalcogenide glasses. These materials have high refractive indices (2.4 to 2.8) and, hence, the light experiences high reflection losses when it enters and exits the fiber (around 32% loss for two faces). Thin film antireflective (AR) coatings can be used to reduce these reflection losses, but they damage at relatively low laser peak power intensities (<0.3 GW/cm^2) compared to the glass (>1 GW/cm^2). This problem worsens when multilayer coatings are used for the purpose of broadband antireflection performance.

The Solution: An alternative approach to reducing the reflection loss is to build a structure into the surface of the optic itself in which the refractive index effectively varies gradually and continuously from air to the value of the bulk. These structures are generally subwavelength and periodic, typically consisting of a collection of identically shaped features, such as graded cones or depressions, that minimize diffraction and

interference effects.[1] The distances between the features, as well as their dimensions, are designed so that they are smaller than the wavelength of light. If these surface structures are periodic, they are often referred to as a "moth eye" surface structure; otherwise, they are called "random" surface structures. The term "moth eye" is derived from nature, where it was observed that the eye of nocturnal insects such as moths reflected little or no visible light regardless of the angle at which incident light struck the eye surface.[2] This phenomenon is now well understood and is attributed to the tiny protrusions on the surface of the eye (Fig. 4). It is now possible to create artificial moth-eye structures in the visible and other wavelengths to significantly reduce the reflection loss from an optical interface between air and a window or a refractive optical element. Oxide glasses with moth-eye surface structures have also demonstrated remarkably higher resistance to damage from high-intensity laser illumination[3] when compared to the glasses with AR coatings. This bodes well for transmitting high-power mid-IR laser energy through suitable structures produced on the endfaces of IR fibers.

Basic Theory: It is important to design and model these antireflective microstructures for the chalcogenide glasses to identify the shape and height of the features that will minimize reflection losses in the infrared region. Two basic guidelines have been clearly established in the literature: the period of the pattern needs to be smaller than the shortest wavelength in the range of interest, and the height of the features needs to be about half of the largest wavelength in the range of interest. A simple model that yields good results is the effective index method, in which the antireflective structure is sectioned into thin slices and light transmission is estimated at each interface. The key point is that each slice contains a different ratio of air and chalcogenide glass, and this ratio changes continuously and smoothly from the top to the bottom of the microstructure. We used this model to design a suitable AR structure for the IR fibers.

Experimental Details: Typically, subwavelength periodic patterns can be obtained directly in the material through photo- or e-beam lithography and etching, or through an embossing approach in which the desired structure is first built in a robust material (such as metal shim) that is then used to replicate the structure in the desired material. Given the practical ease of the embossing method as previously demonstrated in stamping vinyl records, we built a specialized chamber to allow for alignment and stamping of the fiber against the shim (Fig. 5). Temperature was used to control the glass viscosity, which in turn dictated the pressure required to stamp the characteristic features onto the surface of the fiber.

The stamping process was correlated with fiber transmission measurements before and after the embossing process. We compared the measured transmission at a single wavelength (3.39 μm) available from a standard HeNe laser to that obtained over the full wavelength range of interest (2 to 5 μm) using an FTIR spectrometer.

Results: Figure 6 shows an infrared fiber cable that has been stamped on both endfaces. (A) and (B) highlight two different types of features that have been demonstrated: (A) shows a positive moth-eye structure with glass protrusions, and (B) shows a negative moth-eye structure with depressed features. These structures have reduced reflection losses so that the transmission through the cable has increased from 68% to over 90%, and furthermore, the transmission was improved over a large spectral bandwidth (2 to 5 μm). In addition, the fiber cable has successfully transmitted the full output power without damage from an infrared laser used in missile protection systems. With optimized design of the structure, it will be possible to further improve performance and demonstrate transmission above 95% over the full range of interest.

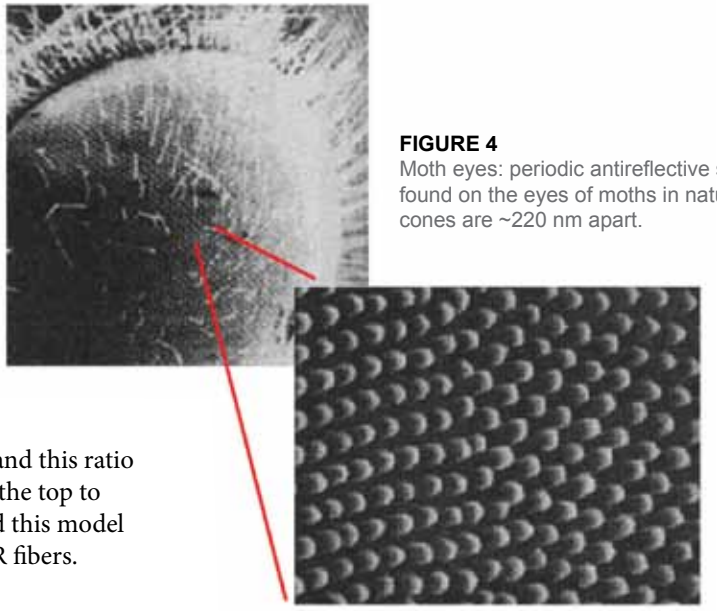

FIGURE 4
Moth eyes: periodic antireflective structures found on the eyes of moths in nature. The cones are ~220 nm apart.

[Sponsored by ONR]

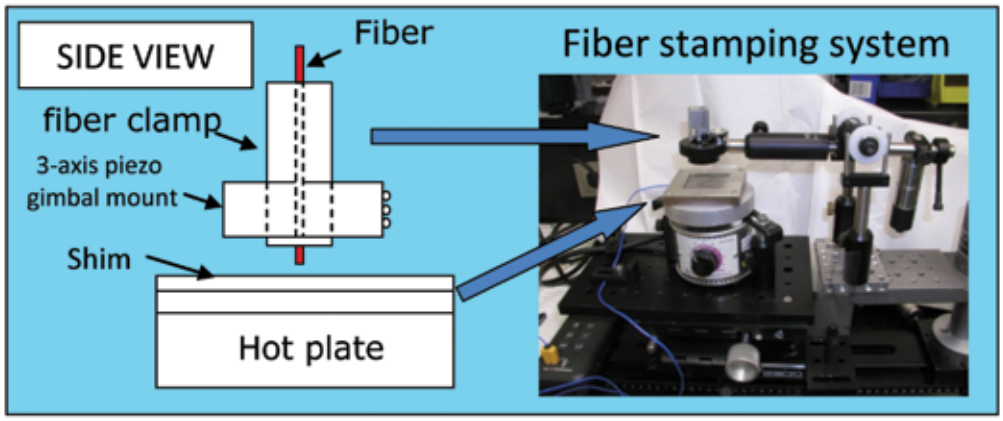

FIGURE 5
A stamping system designed to emboss the antireflective moth-eye structure onto the endface of infrared fibers using a custom-made metal shim.

FIGURE 6
An embossed flexible IR fiber cable with two examples of structures that can be stamped onto the fiber endface: (A) positive moth-eye structure with glass protrusions and (B) negative moth-eye structure with depressed features.

References

[1] J.J. Cowan, "Aztec Surface-relief Volume Diffractive Structure," *J. Opt. Soc. Am.* **7**, 1529 (1990).

[2] P.B. Clapham and M.C. Hutley, "Reduction of Lens Reflexion by the 'Moth Eye' Principle," *Nature* **244**, 281 (1973).

[3] W.H.E. Lowdermilk and D. Milam, "Graded-index Antireflection Surface for High-power Laser Applications," *Appl. Phys. Lett.* **36**, 891 (1980).

Broad-Spectrum Pathogen Surveillance

A.P. Malanoski, T.A. Leski, L. Cheng, Z. Wang, D.A. Stenger, and B. Lin
Center for Bio/Molecular Science and Engineering

Introduction: A comprehensive resequencng microarray, the Tropical and Emerging Infections (TessArray® RPM-TEI 1.0 array), has been developed to identify and distinguish between biothreat organisms of interest and genetically close, related species. The approach was confirmed from testing a subset of target organisms, such as Ebola viruses and Lassa viruses, at the U.S. Army Medical Research Institute of Infectious Diseases (USAMRIID) at Ft. Detrick, Maryland. Most potential biothreat organisms are endemic in some part of the world. Using the resequencing pathogen microarray (RPM) for detection in locations such as West Africa can support indigenous monitoring as it provides sequence information. An ongoing collaboration with Njala University aims to establish a broad-spectrum pathogen surveillance capability in the Republic of Sierra Leone, West Africa, using RPM technology combined with a geographic information system (GIS). This has the potential to improve public health efforts in an infected area as well as provide monitoring of the changes occurring to a biothreat organism in its natural location.

Background: Monitoring biothreat agents has become an important issue since the anthrax attacks of October 2001. Most potential biothreat organisms are indigenous to some part of the world, such as Lassa and Ebola viruses in parts of Africa, or Hantavirus in South America.[1] This complicates monitoring of biothreat agents, as the target organisms are not fixed but evolving. In order to mitigate this risk, it is critical to monitor target organisms in their natural environment as part of any pathogen surveillance. In addition, these organisms pose a serious threat not only to regions that are not normally subjected to their presence but also to local populations that are regularly exposed to them. It becomes clear that it is essential to monitor pathogens in their indigenous environment, so that we can gain understanding of the natural reservoir, transmission mode, and the epidemic and temporal dynamics of the organisms. Furthermore, monitoring of biothreat agents in remote populations can be integrated with local surveillance needs if the testing method provides sufficient information. A diagnostic solution we have developed, high density RPM, which tests for many pathogens simultaneously with high sensitivity and specificity, meets these needs (Fig. 7). The solution has the necessary capability to provide genetic sequence information for the organism(s) detected. A lab has been set up in Bo, Sierra Leone, that has the capability to run this diagnostic.

Resequencing Microarrays: RPM provides these capabilities because of its unique combination of features. The core aspect of this method is the high-density nature of the microarray that allows 1 million individual bases to be interrogated. Groups of contiguous bases (100 to 1000 bases) from a specific virus or bacteria strain can be selected that allow related strains (85% sequence similarity) to also be detected. We recently developed in silico modeling of the platform to improve and simplify the microarray design process.[2] Using this knowledge, it was possible to design in only six weeks an optimal resequencing microarray, TessArray® RPM-TEI 1.0, for the detection of most Centers for Disease Control and Prevention (CDC, Atlanta, Georgia) category A, B, and C biothreat agents. Validating most of the array with the actual organisms would require a biosafety level 3 facility, which would be costly and time consuming. An alternative using sythentic targets was used to validate the microarray. Overall, the testing results of RPM-TEI 1.0 arrays, performed using target sequences matching the sequence used to generate the microarray probes, demonstrated excellent detection capabilities of RPM for biothreat agents. A number of genetically diverse

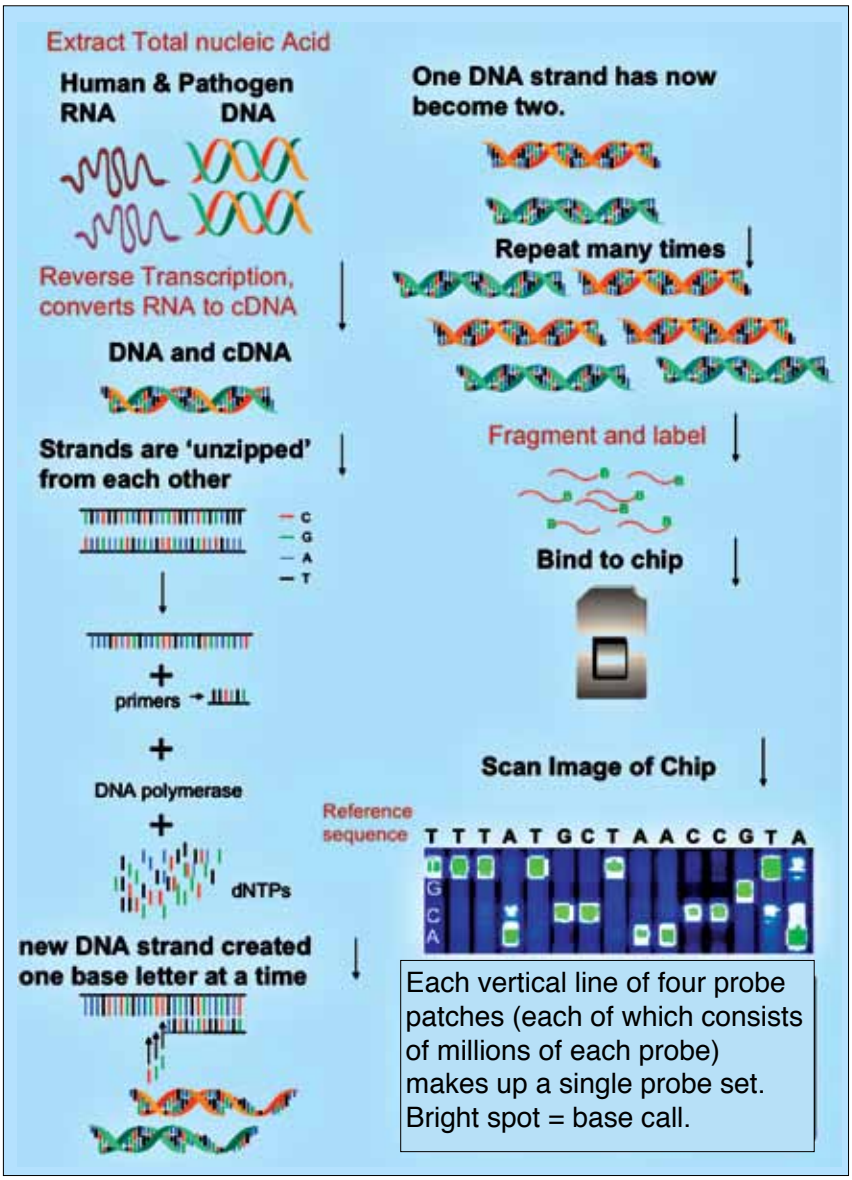

FIGURE 7
Schematic flow diagram of the RPM diagnostic. Total nucleic acids are extracted from a sample, then amplification is carried out to increase the detection sensitivity of the target of interest. Amplified products are subjected to fragmentation and labeling before being hybridized to the microarray. Hybridized microarrays are processed and then scanned to generate the images, which are analyzed to determine a sequence.

viruses were used to confirm these capabilities with experiments conducted in the Virology Division of USAMRIID and carried out according to a standard protocol for testing unknown samples (Table 1).

Sierra Leone: This project aims to create a pathogen surveillance GIS that will use diagnostic data from RPM arrays at Mercy Hospital in Bo, Sierra Leone. Pathogen surveillance must keep track of many factors, such as how a pathogen is transmitted (vector), antibiotic resistance, where it originates, and what it is (biotype/serotype), which have geographic and temporal components that can naturally be stored and related to each other in a GIS. However, implementing a disease-surveillance GIS in Sierra Leone is greatly complicated by the absence of both fine-scale maps in Sierra Leone and the conditions at Mercy Hospital. Power, communications, and computer resources are all required to properly run the RPM diagnostic and to integrate the results into a GIS system. As part of equipping the lab at Mercy Hospital with the RPM platform, a C-band satellite dish was installed, a battery system interfaced with diesel and solar units was set up to provide hybrid power and independence from a single energy source, and the various equipment required for the platform were installed. Collaborators from Njala University have used GPS units to start filling in the missing map information (Fig. 8).

Conclusion: The RPM technology, with its capability of simultaneously testing for many pathogens while providing sequence information, makes it ideal for use where many pathogens have similar initial symptoms and early detection is important. Engaging nations in Africa, Asia, and South America, where many biothreat agents are native, in using this technology provides advanced tools to support their own efforts to improve public health while providing important information for protecting against biothreat agents.

Acknowledgments: The funding for developing the RPM-TEI 1.0 array was provided by the Office of Naval Research. We also appreciated partial support from Tessarae, LLC through a Cooperative Research and Development Agreement (NCRADA-NRL-06-406). The assistance provided by Drs. Sofi Ibriam and Mahamed Aitichou, and Mr. Justin P. Hardick, Ms. Sarah Strand, and Ms. Raquel Abella during the validation of RPM-TEI chips was also greatly appreciated. We are also grateful for the support provided by the Office of the Secretary of Defense (OSD) Coalition Warfare Office for the "Pathogen Surveillance in West Africa" project. Luke Cheng was supported through the Department of Navy (DoN) Science and Engineering Apprenticeship Program (SEAP).

[Sponsored by ONR, OSD, and Tessarae LLC]

References

[1] D.G. Bausch, A.G. Sprecher, B. Jeffs, and P. Boumandouki, "Treatment of Marburg and Ebola Hemorrhagic Fevers: A Strategy for Testing New Drugs and Vaccines under Outbreak Conditions," *Antiviral Res.* **78**(1), 150–161 (2008).

[2] A.P. Malanoski, B. Lin, and D.A. Stenger, "A Model of Base-call Resolution on Broad-Spectrum Pathogen Detection Resequencing DNA Microarrays," *Nucleic Acids Res.* **36**(10), 3194–3201 (2008).

TABLE 1—Selected Agents Tested Using TessArray RPM-TEI 1.0 Array

Organism	Taxon	Concentration	RPM Result
Ebola Zaire	Filoviridae	1 – 10^{-4} ng	Zaire Ebola virus strain Zaire 1995
Ebola Reston		1 – 10^{-3} ng	Reston Ebola virus strain Pennsylvania
Ebola Ivory Coast		10^{-1} ng	Cotê d'Ivoire Ebola virus
Ebola Zaire strain Mayinga		10^{-1} ng	Zaire Ebola virus strain Mayinga
Marburg Ravn		10^{-1} ng	Lake Victoria Marburg virus - Ravn
Marburg Musoke		10^{-1} ng	No detection
Marburg Ci67		10^{-1} ng	Marburg virus strain M/Germany/Marburg/1967/Ratayczak
Lassa Josiah	Arenaviridae	1 – 10^{-3} ng	Lassa virus strain Josiah
Lassa Z148		1 – 10^{-3} ng	Lassa virus strain Z148
Lassa Acar		10^{-1} ng	Lassa virus
Lassa Weller		10^{-1} ng	Lassa virus strain Weller
Lassa Pinneo		10^{-1} ng	Lassa virus

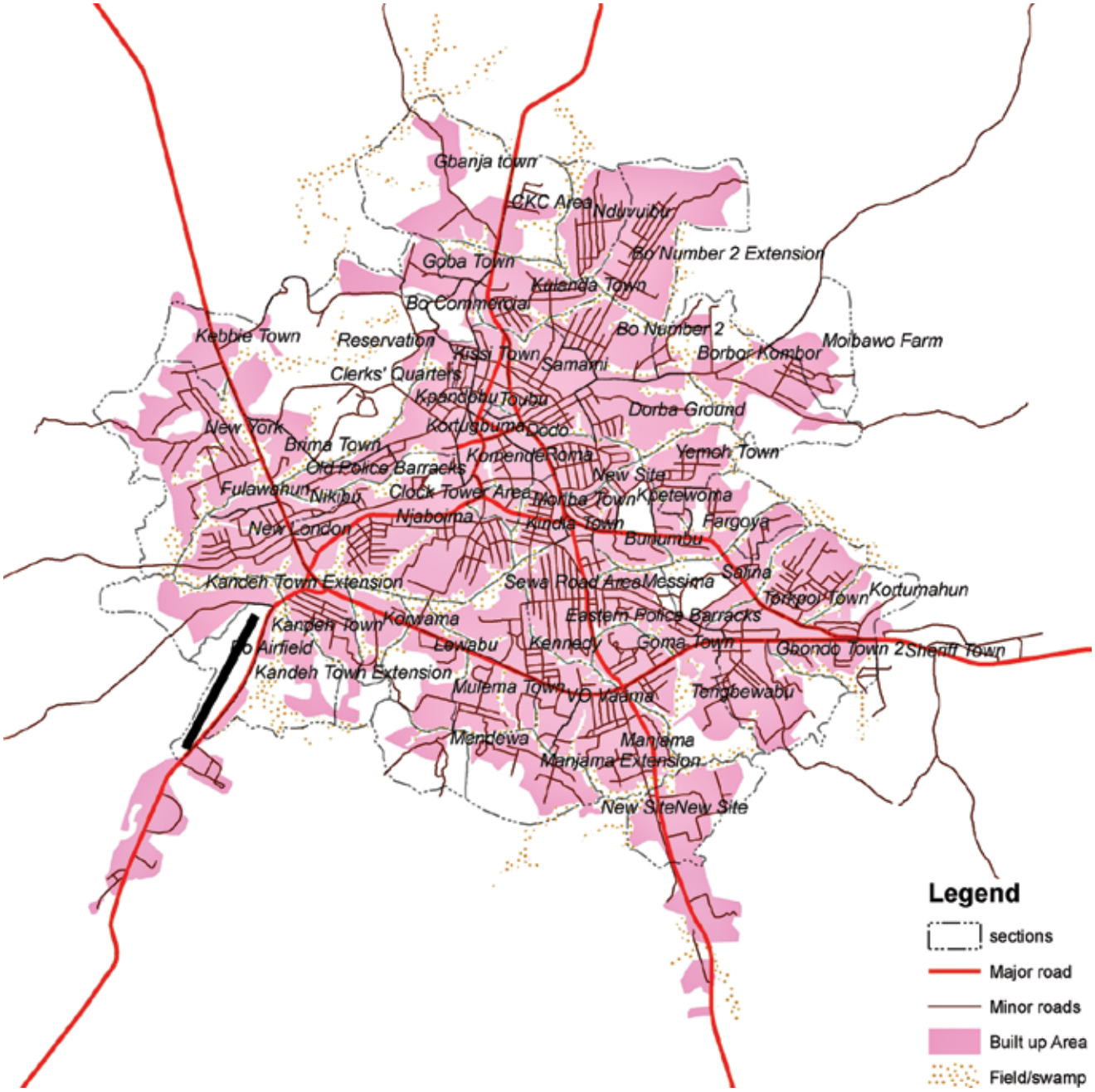

FIGURE 8
Map of Bo, Sierre Leone. This image was made by integrating remote imagery and GPS handheld units. Major and minor roads, built-up areas, fields, and town sections are all indicated.

Plasma Processing of Ion Energy-sensitive Materials

S.G. Walton,[1] E.H. Lock,[1] M. Baraket,[1] D.R. Boris,[1] R.F. Fernsler,[1] S.H. North,[2] C.R. Taitt,[2] J.T. Robinson,[3] F.K. Perkins,[3] and P.E. Sheehan[4]
[1]*Plasma Physics Division*
[2]*Center for Bio/Molecular Science and Engineering*
[3]*Electronics Science and Technology Division*
[4]*Chemistry Division*

Plasma Processing: Plasmas are a critical tool for the production and modification of materials. These partially ionized gases comprising electrons and positive ions can create or modify large areas with precision down to the nanoscale. Consequently, plasmas have been the semiconductor industry's tool of choice to produce the complex circuitry found in the electronic devices we take for granted. Every plasma has its own profile of reactive species including electrons, ions, excited neutrals, reactive neutral fragments (radicals), and photons. This profile depends considerably on the background gas and can be adjusted precisely. By adjusting this profile, the plasma will remove material, deposit material, or change the chemical makeup of the surface to which it is exposed. Despite a string of successes, serious concerns remain over the use of plasmas in producing and modifying materials used in next-generation electronic, sensing, and energy applications. More specifically, ions with large kinetic energies can produce unwanted effects. For polymers, ion-induced surface roughness can render the material unusable, and in the case of monolayer films like graphene, etching must be avoided.

The plasma processing system developed in NRL's Plasma Physics Division averts these issues because of its ability to deliver ions with very low kinetic energies (Fig. 9). To understand this, one must recognize that most plasmas are sustained by applying electric fields. The applied field couples mainly to the electrons, increasing their energy so that some fraction of the population is energetic enough to ionize the gas. While the electrons are energetic, the ions remain at or near the background gas temperature. In order to prevent the more mobile electrons from leaving, the plasma self-organizes to maintain a positive potential such that electron losses are reduced. Nearly all of this potential arises at the plasma-substrate interface, and so positive ions impacting the substrate arrive with energies well in excess of the electrons. Our approach to plasma generation uses a high-energy electron beam to ionize, excite, and dissociate the background gas. Because electric fields are not required, the plasma electrons have very little energy and so the plasma potential is small as well. In fact, ions arrive at the surfaces with energies of only a few eV, a value that is at or below the bond strength of polymeric materials and graphene. We have successfully functionalized polymer substrates of interest in biothreat detection and diagnostic technologies and treated graphene for electronics and sensing applications without damaging the material.

Chemical Functionalization of Microtitre Plates: With colleagues in the Center for Bio/Molecular Science and Engineering, we have developed a method for chemically functionalizing commercial, polystyrene microtitre plates to facilitate biomolecule immobilization. The multi-well microtitre plate is a standard

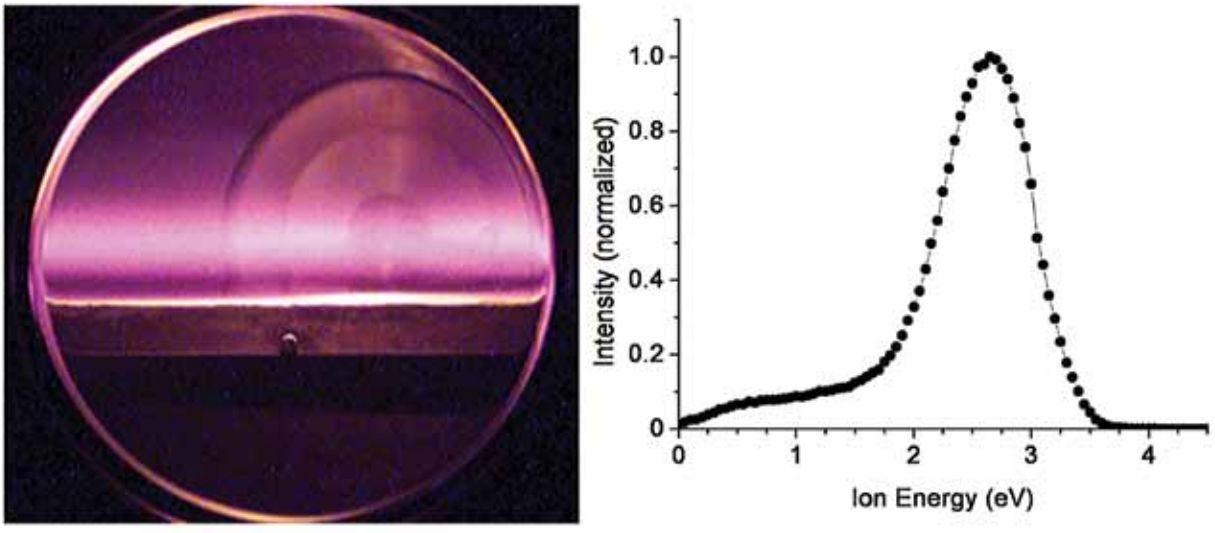

FIGURE 9
NRL's plasma processing system (left) and an ion energy distribution measured at an adjacent processing stage (right). The range of ion energies is below the bond strength of many materials and is a critical feature in the success of the system.

tool used for the development of diagnostic tests and other biological detection schemes. Depending on the target agent, specific "capture" biomolecules are immobilized on the plate surface. While nonspecific adsorption is the most commonly used method for immobilization of proteins, many biomolecules do not retain their enzymatic or binding activities when immobilized in this fashion. Specifically, covalent immobilization allows for a stable and oriented display of these biomolecules. Using our plasma processing system, we introduce chemical functionalities to the plate surfaces, which allow for virtually any type of covalent attachment chemistry without changing the surface morphology. In Fig. 10, we demonstrate differential binding properties of a bacterial biomarker, lipopolysaccharide (LPS), to a variety of antimicrobial peptides (AMPs) immobilized onto plate surfaces that have been treated with plasma (bottom) and those that have not (top). Although the example of Fig. 10 is specific to oxygen, the plasma-based approach is flexible and allows us to introduce a variety of chemical moieties for covalent attachment.

Chemical Functionalization of Graphene:
Graphene is a single monolayer of sp^2 bonded carbon, with superlative electrical, mechanical, and thermal properties. However, to increase the range of potential graphene-based applications, precise control over surface functionalities is required. With colleagues in the Chemistry and Electronics Science and Technology Divisions, we have developed an approach that can decorate the surface of graphene with various functional groups without adversely disrupting the graphene honeycomb structure. Figure 11 shows chemical and structural characteristics before and after adding oxygen functional groups. The oxidized graphene has distinct chemical signatures associated with the addition of oxygen as well as a significantly increased D-peak, indicating the transformation from sp^2 to sp^3 carbon. However, the sp^2 carbon and the graphitic-induced G band remain. Importantly, after high-temperature annealing to remove the functionalities, the pretreatment characteristics are recovered, indicating little or no damage to the graphene structure as a result of the treatment. Here again, the

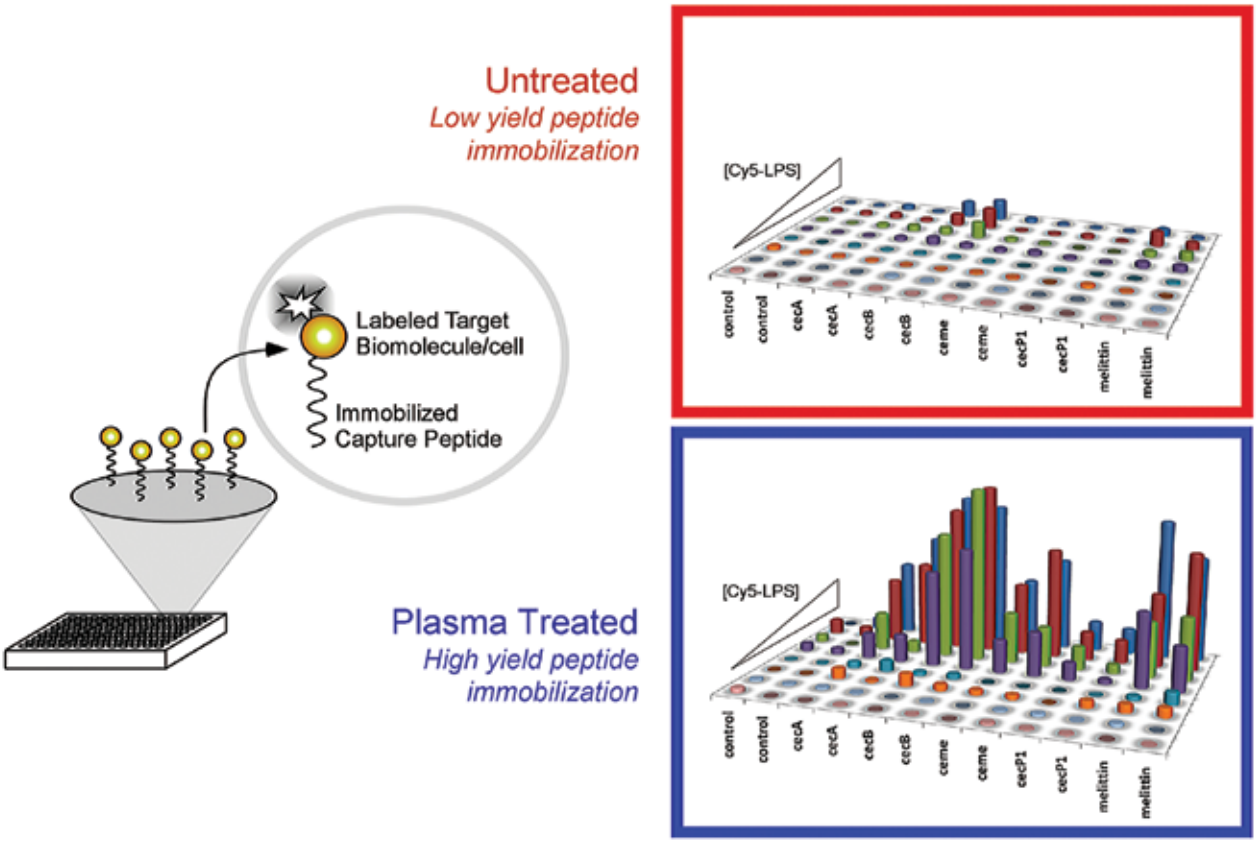

FIGURE 10
Fluorescence from untreated (top) and plasma treated (bottom) microtitre plates indicating the binding of a fluorescently labeled bacterial biomarker, lipopolysaccharide (LPS), to a variety of antimicrobial peptides. Plasma treatment introduces chemical moieties that promote the covalent immobilization of peptides, thereby increasing the LPS capture yield and the associated signal strength by up to 40 times compared to the untreated plates.

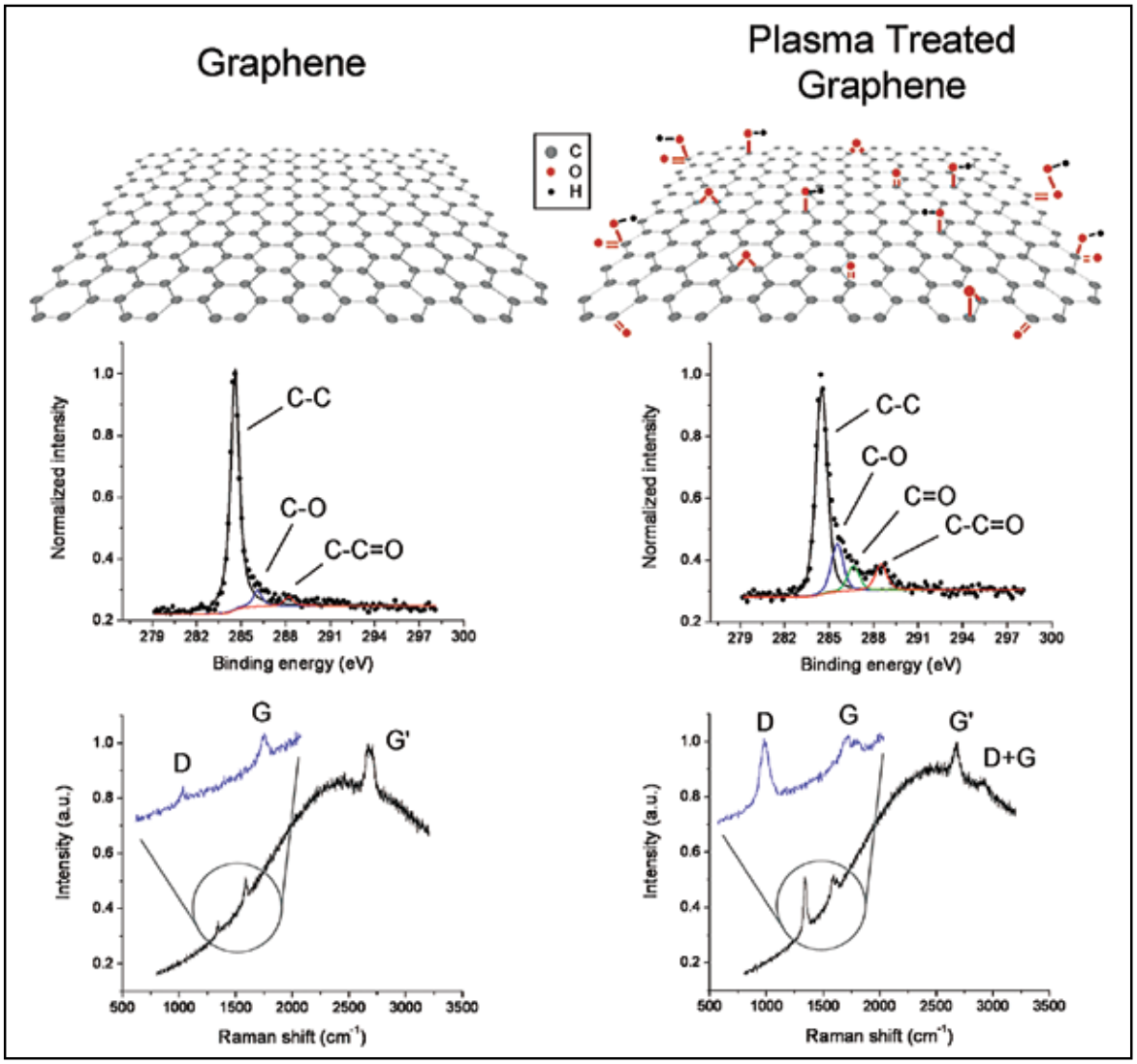

FIGURE 11
A representation of graphene functionalization (top) along with supporting surface diagnostics. X-ray photoelectron spectroscopy (XPS) measurements (middle) show an increase in the oxygen functionalities bound to carbon after exposure to an argon/oxygen plasma. The presence of those species alters the carbon bond structure, as indicated by the increase in the D band signal in the Raman spectrum (bottom).

system's flexibility enables us to tailor the functional group by simply changing the operating gas mixture.

[Sponsored by NRL/ONR and DTRA]

Standoff Detection of Trace Explosive Residues by Resonant Infrared Photothermal Imaging

C. Kendziora,[1] R.A. McGill,[1] R. Furstenberg,[1] M. Papantonakis,[1] V. Nguyen,[1] G. Hubler,[1] and J. Stepnowski[2]
[1]*Materials Science and Technology Division*
[2]*Nova Research Inc.*

Counter-IED Motivation: Motivated by improvised explosive device (IED) and homeland security concerns, explosives detection is a critical research area for the Navy, the Department of Defense (DoD), and the Department of Homeland Security (DHS). An emerging thrust is to potentially replace point detection of trace residues (which requires physical contact) with standoff capability from a safe distance. Ideally, a standoff technique should be safe to use around people, nondestructive, selective, rapid, and adaptable to new types of threats. NRL's Materials Science and Technology Division has demonstrated a novel resonant infrared (IR) photothermal approach that has the potential to meet these goals. In this technique,

light of a specific infrared wavelength is directed to the surface of interest and the thermal response is viewed with an infrared camera. Comparing the thermal image as a function of incident wavelength with the absorption spectrum of explosives reveals the presence and location of trace residues. By varying the incident wavelength, other analytes of interest (e.g., drugs and chemical agents) could also be imaged. Field testing of an NRL-built system was successfully performed at the Yuma Proving Ground in Yuma, Arizona.

Infrared Signature Based Technical Approach: The infrared region of the electromagnetic spectrum between 2 and 12 μm is often referred to as the "fingerprint region" for chemical identification because the patterns of absorption bands are highly material specific. Figure 12 illustrates the IR transmission for three explosives analytes of interest — RDX, TNT, and DNT — and water vapor in air at atmospheric pressure.[1] This selective absorption property is exploited in the NRL Remote Explosives Detection (RED) approach by shining light from an infrared quantum cascade laser (QCL) at a wavelength that is selectively absorbed by trace explosives on the surface of interest. Due to the low vapor pressure of explosives, these traces can persist in particle form for months or longer.

Figure 13 shows the schematic diagram for the NRL RED technology.[2] The 6.25 μm wavelength is selectively absorbed by the nitrogen–oxygen stretch vibration common to most high explosives. The 6.25 μm light is transmitted through humid air due to a narrow gap in the water vapor absorption spectrum. Additional laser wavelengths can be added to increase sensitivity and selectivity, or to detect other analytes of interest. Signal collection is performed in the long-wave IR (LWIR) transparent region of the spectrum from 8 to 12 μm. The figure also shows an example differential image (laser "on" minus laser "off") where both TNT and RDX are detected using 6.25 μm wavelength light from a QCL.[3] The red circle indicates the area illuminated by the beam.

Field Testing at Yuma Proving Ground: A multidisciplinary team of physicists, chemists, and engineers from the Division designed, assembled, and field-tested a cart-based system to test the RED technology under a variety of ambient parameters, including temperature, sunlight, humidity, dust, wind, and standoff distance.[4] Figure 14 shows the assembled RED cart system during testing at the Yuma Proving Ground. The red arrow in the figure traces the approximate path of the invisible IR laser beams from the cart to the sample tripod 10 m away. The cart system actually features four lasers (two on resonance and two off resonance) to increase the detection sensitivity and selectivity. The beams are collimated at a 12 mm diameter to optimize use of the available laser power. The laser output powers were in the eye-safe (Class 1) range so that users and observers did not have to wear laser goggles. The thermal imager used on the cart was an inexpensive uncooled bolometer array. The collection optic was a standard commercial germanium lens.

The experiment consisted of directing the laser beam (and co-aligned collection optics) toward a surface of interest using a mirror gimbal. A sequence of four laser pulses took approximately 1 s while the thermal images were collected. Comparing the frames with the laser on to those with the laser off yielded the signal due to the RED process. During this testing, the explosives TNT, RDX, PETN, C4, Tetryl, Comp B, PBX4, and PE4 were successfully detected as far as 30 m away. This distance is not a fundamental limitation for the technique, and improvements to the system are ongoing.

This field test demonstrated that the RED technique is not limited by daylight, variable temperature, humidity, or sand. It was able to detect all eight explosives species tested at 10 m or greater distance using eye-safe laser powers. The capability to perform standoff detection of trace explosives using eye-safe lasers is of great importance in the counter-IED mission for Navy, DoD, and DHS applications. This technology is being further developed to make the system more compact and rugged, and to increase system sensitivity, selectivity, and standoff distance capability.

[Sponsored by the OSD Rapid Reaction Technology Office and NRL/ONR]

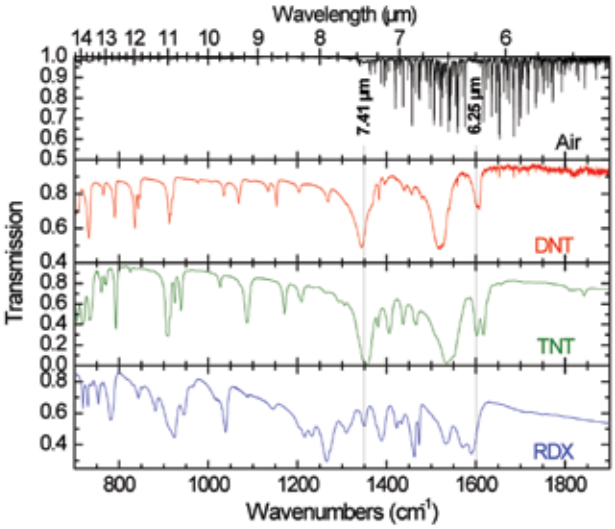

FIGURE 12
The infrared transmission spectra of the explosives RDX, TNT, and the decay product DNT. Dips in the spectra correspond to absorption bands. Absorption bands common among the explosives, such as those shown at 6.25 and 7.41 μm, are highlighted with vertical lines.

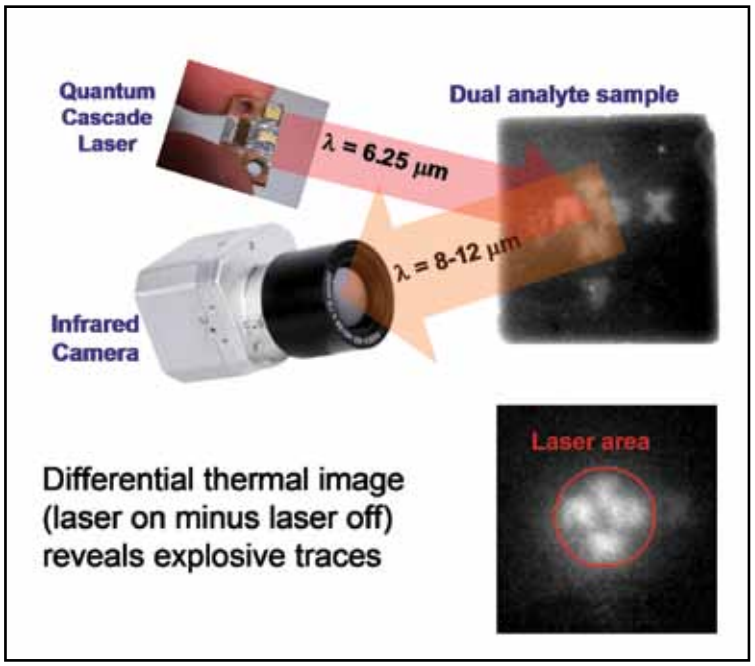

FIGURE 13
The RED technology. An IR beam from the QCL is selectively absorbed by the trace explosives on a surface, causing a slight heating. This heat signal is detected and imaged using an IR camera.

FIGURE 14
The NRL cart system during testing at the Yuma Proving Ground. The sample tripod is positioned at 10 m standoff distance. The red arrow illustrates the approximate path of the invisible infrared beam.

References

[1] R. Furstenberg, C.A. Kendziora, J. Stepnowski, S.V. Stepnowski, M. Rake, M.R. Papantonakis, V. Nguyen, G.K. Hubler, and R.A. McGill, "Stand-off Detection of Trace Explosives via Resonant Infrared Photothermal Imaging," *Appl. Phys. Lett.* **93**, 224103 (2008).

[2] R.A. McGill et al.,"Detection of Chemicals With Infrared Light," U.S. Patent Application No. 12/255,103, filed Oct. 21, 2008, Publication No. US2010/0044570 A1, Feb. 25, 2010.

[3] M.R. Papantonakis, C. Kendziora, R. Furstenberg, S.V. Stepnowski, M. Rake, J. Stepnowski, and R.A. McGill, "Stand-off Detection of Trace Explosives via Resonant Infrared Photothermal Imaging," *Proc. SPIE* **7304**, 730418-8 (2009).

[4] R. Furstenberg, C. Kendziora, M. Papantonakis, S.V. Stepnowski, J. Stepnowski, V. Nguyen, M. Rake, and R.A. McGill, "Stand-off Detection of Trace Explosives by Infrared Photo-thermal Spectroscopy," *IEEE Conf. on Technol. for Homeland Security*, 2009, **978-1-4244-4179-2**, 465–471 (2009).